sciheritage

Koopman-Lifted Observability and Optimal Excitation for Dissolution-Buffered Gas Influx Identification in Managed Pressure Drilling

Agus Setiawan[1], Bagus Mahendra[2], Yoga Firmansyah[3]

[1]Universitas Maritim Raja Ali Haji, Jalan Raya Dompak, Tanjungpinang 29115, Kepulauan Riau, Indonesia
[2]Universitas Tadulako, Jalan Soekarno Hatta Km. 9, Palu 94148, Sulawesi Tengah, Indonesia
[3]Banjarmasin, Indonesia

ABSTRACT Drilling operations conducted within narrow pressure windows increasingly rely on managed pressure drilling to regulate annular pressure through choke and pump actuation. Yet, early gas influx identification remains challenging because surface measurements are aggregated, boundary actuation is persistent, and fluid properties evolve with pressure and temperature. In oil-based and synthetic-based systems, a substantial fraction of invading gas may dissolve and induce liquid swelling, altering pit-volume and pressure signatures without immediate formation of a dominant free-gas phase. This paper develops an operator-theoretic identification framework that targets the underlying information limitation directly: the separation of influx, dissolution, and frictional transients is fundamentally an observability problem under constrained excitation. The technical contribution is a Koopman-lifted, control-affine surrogate of dissolution-aware annular hydraulics that enables tractable computation of observability and Fisher-information surrogates in a lifted space while preserving bounded thermodynamic state augmentation. A receding-horizon excitation design is then posed to maximize a risk-weighted information metric subject to bottomhole-pressure constraints and actuator rate limits, yielding control perturbations that are intentionally informative yet operationally admissible. The resulting method produces calibrated posterior contraction rates for influx-rate and depth proxies without assuming that any single sensor signature is uniquely attributable to free gas. Numerical studies show that modest, structured choke perturbations can increase identifiability of dissolution kinetics and influx magnitude in regimes where pit gain alone is ambiguous, and that Koopman-lifted information metrics remain stable under property-model uncertainty and sensor bias, supporting real-time deployment as an observability-aware layer alongside conventional control.

I. Introduction

Gas influx identification in drilling is often treated as a pattern recognition task applied to pit volume, standpipe pressure, or flow-out discrepancies [1]. That framing can be adequate in benign regimes, but it becomes structurally unreliable when the operating window is narrow, actuation is continuous, and fluid systems are thermodynamically active. Managed pressure drilling modifies the boundary conditions of the annulus on purpose: choke backpressure, pump ramps, and flow-out control reshape the internal pressure distribution and, consequently, reshape the mapping from downhole states to surface signals. Under these circumstances, there is rarely a single signature that is both sensitive and specific to a gas influx, and false separations between "control transients" and "kick transients" arise because both are generated by the same governing dynamics under different inputs. A robust inference approach must therefore confront an underlying fact: the system is only partially observed, and identifiability is governed as much by excitation and sensor geometry as by the fidelity of any particular forward simulator.

The difficulty intensifies when dissolution and swelling are relevant [2]. If a portion of the invading gas dissolves into the liquid phase, the free-gas holdup may remain small while the liquid expands, decreasing its density and increasing its volumetric return for a given mass flux. The same surface pit-volume trajectory can then be generated by markedly different internal states: a free-gas-rich annulus with negligible dissolution, or a dissolution-buffered annulus in which the gas inventory is largely dissolved at depth. A purely free-gas interpretation can overpredict surface gas handling

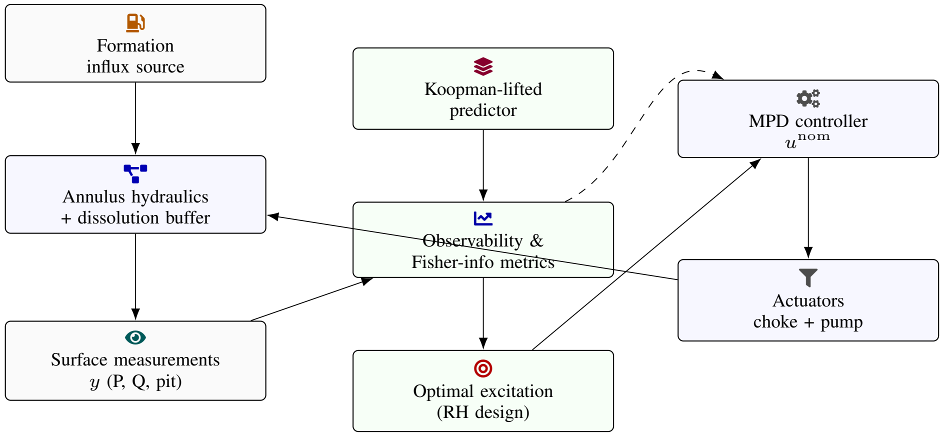

FIGURE 1: Managed-pressure drilling (MPD) closed-loop architecture with an observability-aware identification layer. Small, admissible excitation perturbations are designed around a nominal MPD trajectory to increase information about dissolution-buffered influx parameters while respecting operational constraints.

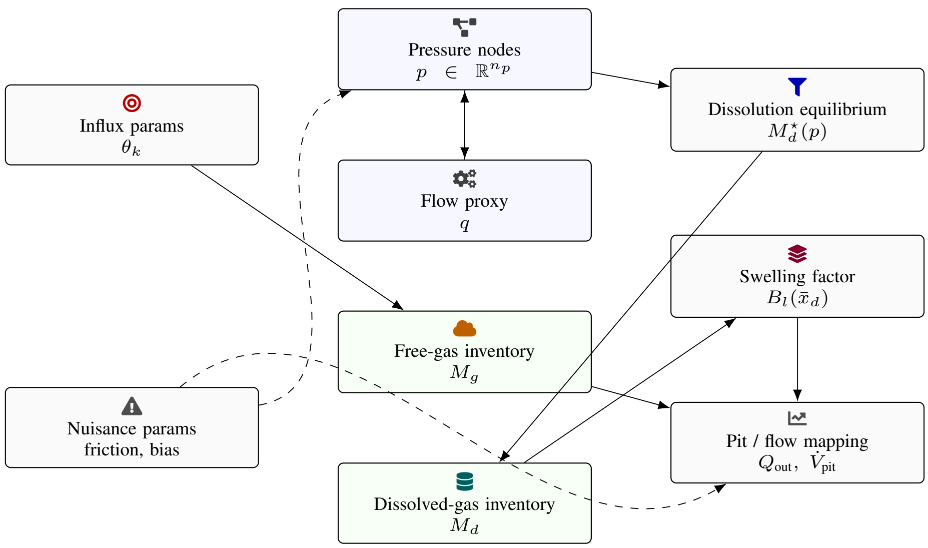

FIGURE 2: Reduced dissolution-aware annular model structure. The state includes pressure nodes, flow proxy, free and dissolved gas inventories, and a swelling-induced volumetric mapping, enabling explicit representation of ambiguity between dissolution-buffered swelling and free-gas-driven transients.

risk, while a purely dissolution-buffered interpretation can underpredict the rate at which free gas might emerge if pressure conditions change. The ambiguity is not a detail; it is a direct consequence of the physics that couple pressure, solubility, and transport, and it persists even with low sensor noise if the operational inputs do not excite the distinguishing dynamics. In this sense, early influx identification is not merely an estimation problem but an observability problem, and the operational lever available to improve observability is controlled excitation that remains within safety constraints.

Thermodynamic modeling has made the dissolution mechanism operationally computable [3]. Manikonda et al. (2020) and Manikonda et al. (2021) introduced the first thermodynamic modeling framework designed to predict how gas kicks dissolve in oil-based drilling fluids [4] [5], linking pressure–temperature conditions to dissolved-gas content and associated volume change in a manner relevant to pit-volume interpretation. Such modeling suggests that dissolution can be treated as a state variable rather than as an ad hoc correction, but it also raises a new question: even if dissolution can be modeled, can it be identified from surface signals in real time, and if so under what excitation patterns? A second modeling complication is that uncertainty in PVT and transport closures can compete with influx effects in the same outputs [6] [7] [8]. Property uncertainty that is small in steady calculations can become significant in transient inference because compressibility and frictional gradients amplify systematic deviations. Sleiti et al.

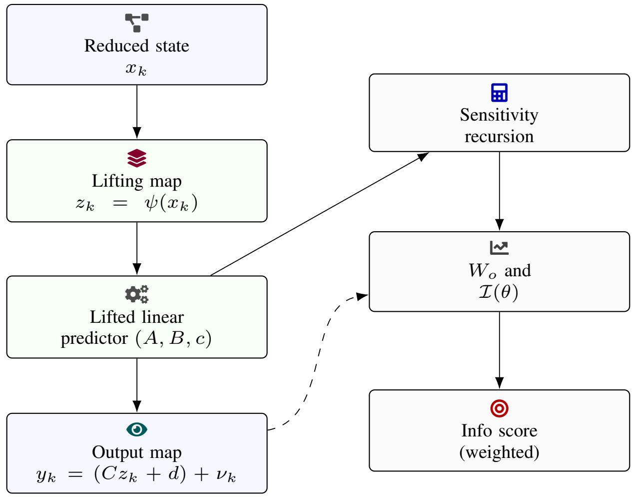

FIGURE 3: Koopman-lifted surrogate pipeline for online observability and information computation. Nonlinear physics are embedded in the lifting map, while linear evolution in lifted coordinates enables fast Gramian- and Fisher-information-based metrics.

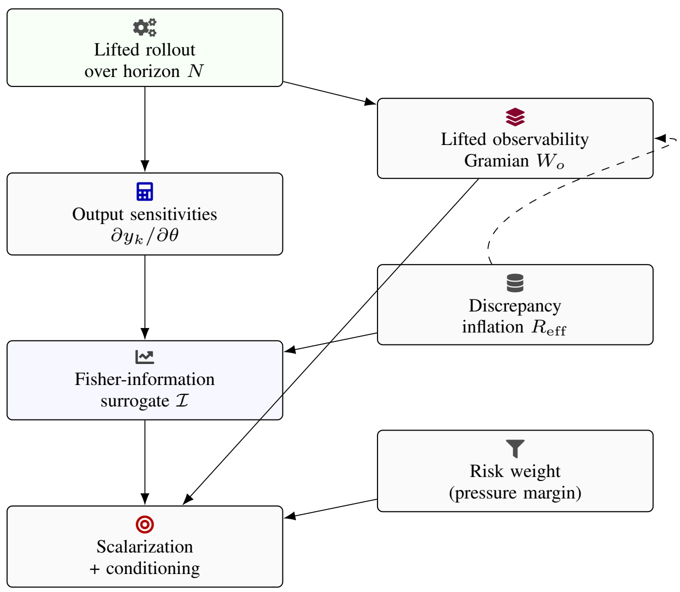

FIGURE 4: Online information metric construction in lifted space. Sensitivities provide Fisher-information surrogates, while a lifted observability Gramian and discrepancy-aware noise inflation yield conservative, operationally meaningful scores for excitation selection.

(2021) evaluated common correlations used in kick-related modeling and reported residual errors that can remain on the order of a few percent even for comparatively accurate high-temperature and high-pressure gas-viscosity formulations, including 3.50% to 4.45% ranges in average absolute relative error for selected density-based models, underscoring that small closure errors can materially influence transient pressure predictions and thus identifiability [9] [10].

Conventional approaches respond to partial observability by adding more estimation machinery, for example by increasing the dimension of a Bayesian filter, using larger ensembles, or fitting flexible surrogates. Those methods can improve numerical robustness, but they do not change the information content of the measured data. If the system is poorly observable under the applied inputs, the estimator will remain ambiguous, and any apparent confidence can be an artifact of modeling assumptions rather than a reflection of information. The goal of this paper is to shift the emphasis from estimation mechanics to information structure by developing an observability-aware identification framework that explicitly designs admissible excitation to maximize information about influx parameters and dissolution states while respecting bottomhole-pressure and operational constraints.

Achieving this goal requires three ingredients that are not typically combined in drilling inference workflows. First, one needs a control-oriented dynamical representation that

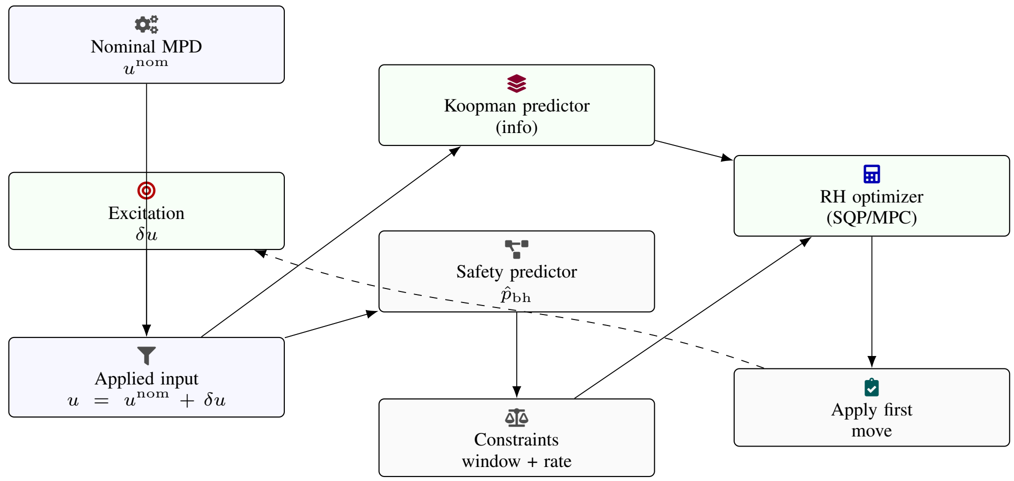

FIGURE 5: Receding-horizon excitation design under pressure-window safety. The optimizer balances information gain against input penalties while enforcing conservative bottomhole-pressure and actuator constraints, then applies the first perturbation and repeats.

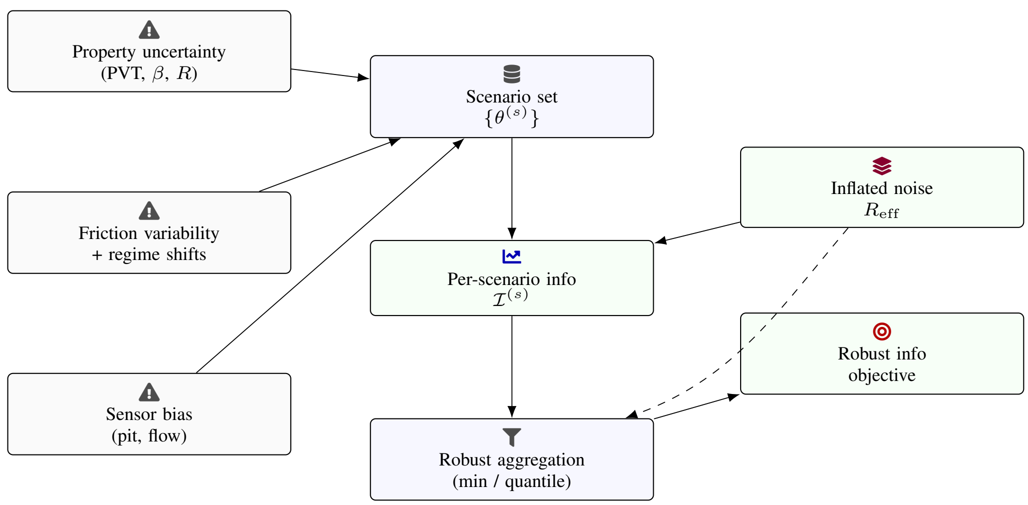

FIGURE 6: Robust information evaluation under uncertainty and bias. Scenario-based aggregation and discrepancy-aware noise inflation produce conservative objectives that reduce sensitivity to surrogate mismatch and nuisance-parameter confounding during excitation design.

includes dissolution and swelling as states, because otherwise the designed excitation cannot target the distinguishing dynamics [11]. Second, one needs a tractable method to compute observability and information metrics online, because excitation design must operate at the same cadence as control and monitoring. Third, one needs an optimization formulation that balances information gain against operational risk and disruption, because the excitation must be safe and acceptable in the operational context. The proposed approach combines these ingredients by using an operator-theoretic surrogate based on Koopman lifting to construct a linear predictor in a lifted space, enabling fast computation of observability Gramians and Fisher-information surrogates, and by embedding these metrics within a constrained receding-horizon excitation design.

The central thesis is that Koopman-lifted observability metrics provide a practical bridge between physics-based modeling and information-theoretic experiment design for dissolution-buffered influx identification. Koopman operator methods approximate nonlinear dynamics by linear evolution of observables, which can be constructed to include physically meaningful nonlinear functions of the state. This yields a representation that is linear in the lifted coordinates but retains nonlinear dependence through the lifting map [12]. In the present context, lifting is used not as a generic surrogate but as a structured device: the lifted coordinates explicitly include bounded representations of dissolved fraction and swelling, pressure-dependent compressibility proxies, and conservative inventories that reflect transport and solubility coupling. Once a linear predictor is available in lifted space, classical observability and information metrics become tractable, and one can pose excitation design problems that would be intractable with the full nonlinear distributed model.

TABLE 1: Reduced annular state variables and observability roles

Group	State(s)	Symbol	Observability role
Pressure field	Pressure nodes	$p(t) \in \mathbb{R}^{n_p}$	Capture hydrostatic, frictional and compressible response to choke and pump actuation.
Mixture flow	Mixture-flow proxy	$q(t)$	Links actuation to pressure drops and flow-out signatures.
Free gas	Integrated free-gas mass	$M_g(t)$	Encodes influx magnitude and exsolution, affecting pressure and flow-out.
Dissolved gas	Dissolved mass, average fraction	$M_d(t),\ \bar{x}_d(t)$	Governs swelling and density changes that drive pit-volume trajectories.
Near-surface gas	Free-gas fraction proxy	$\bar{\alpha}_g(t)$	Relates to surface gas handling indicators and slip timing.

TABLE 2: Inputs, outputs, and disturbances in the reduced model

Category	Quantity	Symbol	Description
Control input	Choke actuation	$u_{\mathrm{ch}}(t)$	Modulates annular back-pressure and pressure transients.
Control input	Pump rate	$u_{\mathrm{p}}(t)$	Sets bulk circulation and contributes to frictional losses.
Disturbance	Influx mass rate	$\dot{M}_{\mathrm{in}}(t)$	Parameterized kick inflow entering the annulus.
Disturbance	Process disturbance	$\xi(t)$	Aggregated unmodeled dynamics in state evolution.
Measured output	Surface pressures	$y_p(t)$	Casing and standpipe pressure proxies.
Measured output	Flow-out and pit volume	$Q_{\mathrm{out}}(t),\ V_{\mathrm{pit}}(t)$	Volumetric return and inventory change signals.
Measurement error	Noise and bias	$\varepsilon(t)$	Sensor noise and quasi-static offsets.

The technical contributions of the paper are organized around this thesis. A dissolution-aware, control-affine annular model is first formulated in a reduced coordinate representation that preserves the key couplings among pressure, free gas, and dissolved gas. A Koopman-lifted surrogate is then constructed using data generated from that model across admissible operating envelopes, with lifting functions chosen to enforce boundedness and to preserve conservative quantities. Observability is characterized through a lifted Gramian and through a Fisher-information surrogate for selected influx and dissolution parameters [13]. A constrained excitation design is then posed to maximize a risk-weighted information objective under bottomhole-pressure inequality constraints and actuator rate limits, producing safe input perturbations that target the most ambiguous parameter directions. Finally, numerical studies evaluate identifiability improvement, robustness under property uncertainty and sensor bias, and the operational trade-offs introduced by information-seeking excitation.

The remainder of the paper proceeds as follows. The next section develops a dissolution-aware reduced annular model and defines the parameterization of influx and uncertain closures relevant to identifiability. The following section constructs the Koopman-lifted predictor and derives observability and information metrics that can be evaluated online [14]. The next section formulates the constrained ex-

TABLE 3: Dissolution and swelling dynamics in the reduced formulation

Quantity	Representative relation	Physical meaning
Dissolved-gas rate	$\dot{M}_d = \kappa_d\big(M_d^\star(p) - M_d\big) + \eta_d$	Relaxation toward pressure-dependent equilibrium with process error.
Free-gas rate	$\dot{M}_g = \dot{M}_{\text{in}} - \dot{M}_{\text{out}} - \kappa_d\big(M_d^\star(p) - M_d\big)$	Balances influx, outflow, and dissolution/exsolution.
Equilibrium dissolved mass	$M_d^\star = M_d^\star\big(p(t)\big)$	Solubility-driven dissolved inventory at current pressure.
Average dissolved fraction	$\bar{x}_d = M_d/M_l$	Normalized dissolved content for an effective liquid mass.
Swelling factor	$B_l(\bar{x}_d)$	Maps liquid mass flow to volumetric flow and modifies effective density.

TABLE 4: Parameter partition and identifiability targets

Subvector	Physical content	Representative elements	Focus
θ_k	Influx characterization	Onset time τ_k, depth proxy, rate magnitude and shape	Primary target
θ_f	Friction and flow regime	Friction multipliers, smoothing exponents	Nuisance, confounds pressure
θ_s	Slip and near-surface gas	Slip timing proxies affecting $\dot{M}_{\text{out}}$, $\bar{\alpha}_g$	Affects gas-handling risk
θ_d	Dissolution and swelling	κ_d, equilibrium solubility and swelling coefficients	Targeted jointly with θ_k
θ_b	Sensor biases	Pit-volume and flow-out offsets and drifts	Must be separated from swelling effects

citation design and describes how information objectives are balanced against pressure-window and actuation constraints. The subsequent section addresses robustness, including how property uncertainty and sensor bias are incorporated into information metrics without relying on fragile linearizations around a single nominal model. The final technical section reports numerical studies demonstrating how excitation changes posterior contraction rates and reduces ambiguity in swelling-dominated regimes. The paper concludes with implications for real-time monitoring and for integration with managed pressure control workflows.

II. Dissolution-Aware Reduced Annular Model and Identifiability Targets

A full annular simulator with multiphase transport and thermodynamic closure can be computationally intensive, and more importantly it can be structurally ill suited to online observability analysis because its dimension is large and its dynamics are stiff under rapid actuation. The goal in this section is therefore not to reproduce full fidelity, but to define a reduced model that retains the couplings that dominate observability of influx and dissolution states from surface signals [15]. The reduced model acts as the generative system from which Koopman-lifted surrogates are trained and against which excitation design is posed.

The annulus is treated as a one-dimensional conduit aligned with measured depth. The reduced state is built from coarse spatial aggregation rather than fine-grid discretization. Specifically, pressure is represented by a small number of nodes along the annulus, capturing the dominant hydrostatic and frictional structure while allowing pressure-wave effects to be represented in a low-order manner. Gas inventory is represented by an integrated free-gas mass and an integrated dissolved-gas mass, together with a near-surface free-gas in-

TABLE 5: Representative Koopman lifting observables for dissolution-aware dynamics

Group	Example observables	Purpose
Base states	p_i, q, M_g, M_d, $\bar{\alpha}_g$	Preserve original reduced dynamics.
Bounded fractions	$\sigma(\bar{x}_d)$, $\sigma(\bar{\alpha}_g)$	Enforce bounded dissolved and free-gas indicators.
Pressure features	p_i^2, $p_i p_j$, $\sigma(p_i)$	Capture pressure-dependent solubility and compressibility effects.
Inventory couplings	$M_g p_i$, $M_d p_i$, $M_g \bar{x}_d$	Encode interaction between gas inventories and pressure field.
Swelling proxies	$B_l(\bar{x}_d)$, $B_l^2(\bar{x}_d)$	Represent volumetric expansion and density reduction.
Conservative proxies	$M_g + M_d$, smoothed inventory ratios	Approximate conserved totals to improve stability.

TABLE 6: Observability and information metrics in the lifted setting

Metric	Expression (schematic)	Interpretation
Lifted observability Gramian	$W_o = \sum_{k=0}^{N-1} (A^\top)^k C^\top C A^k$	Ability to reconstruct lifted state from outputs.
Output sensitivity	$\partial y_k / \partial \theta$	Local mapping from parameters to measurement changes.
Fisher information	$\mathcal{I}(\theta) = \sum_k (\partial y_k/\partial \theta)^\top R^{-1} (\partial y_k/\partial \theta)$	Expected curvature of log-likelihood.
Log-det objective	$\log\det \mathcal{I}_{\theta_k,\theta_d}$	Volume reduction for influx and dissolution parameters.
Conditioning penalty	$\kappa(\mathcal{I})$ or trace of $\mathcal{I}^{-1}$	Penalizes nearly collinear sensitivity directions.
Risk-weighted score	$\mathcal{J}_{\text{info}} - \gamma\, \text{risk}$	Trades information gain against safety margins.

dicator that influences surface gas handling. Liquid swelling is represented by an effective swelling factor derived from the dissolved-gas state [16]. These choices are motivated by the nature of available measurements: surface pressures, pit volume change, and flow rates are sensitive to integrated inventories and boundary pressures rather than to fine-scale distributions.

Let the reduced state vector be denoted by $x(t) \in \mathbb{R}^n$, consisting of a pressure node vector $p(t) \in \mathbb{R}^{n_p}$, a mixture-flow proxy $q(t)$, an integrated free-gas mass $M_g(t)$, an integrated dissolved-gas mass $M_d(t)$, and a near-surface free-gas fraction proxy $\bar{\alpha}_g(t)$. The dissolved state is also expressed as an average dissolved mass fraction $\bar{x}_d(t)$ defined by $\bar{x}_d = M_d/M_l$ for an effective liquid mass M_l that is treated as slowly varying over the horizon relative to gas inventories. The system is driven by control inputs $u(t)$ representing choke action and pump rate. The modeling objective is to capture how u influences pressure evolution, how pressure influences dissolution equilibrium, how dissolution influences swelling and density, and how these mechanisms together influence pit volume change and surface gas flow.

TABLE 7: Constraints in receding-horizon excitation design

Constraint	Mathematical form (schematic)	Operational role
Bottomhole pressure window	$p_{\min} + m_k \le \hat{p}_{\mathrm{bh},k}(\delta u) \le p_{\max} - m_k$	Enforces safe pressure with conservative margins.
Actuator amplitude	$\delta u_{\min} \le \delta u_k \le \delta u_{\max}$	Limits perturbation magnitude on choke and pump.
Actuator rate	$\|\delta u_k - \delta u_{k-1}\| \le r_{\max}$	Ensures smooth, implementable excitation.
Surface gas proxy	$\hat{\alpha}_{g,\mathrm{surf},k} \le \alpha_{g,\max}$	Avoids excessive near-surface free gas.
Excitation penalty	$\lambda_u \sum_k \|\delta u_k\|^2$	Discourages disruptive control deviations.
Horizon update	Apply first δu_0, shift horizon	Enables adaptation as estimates and conditions evolve.

TABLE 8: Robust information evaluation mechanisms

Mechanism	Implementation	Effect on excitation
Noise inflation	$R_{\mathrm{eff}} = R + R_{\mathrm{mod}}$ using surrogate validation error	Reduces apparent information in poorly modeled regimes.
Scenario evaluation	$\mathcal{I}^{(s)}(\theta)$ over property and friction scenarios	Seeks excitation informative across plausible models.
Bias parameters	Include pit and flow biases in θ_b and sensitivities	Prevents misattributing bias effects to swelling.
Coupled property uncertainty	Bounded, correlated perturbations in resistance/compressibility	Avoids unphysical combinations in robustness analysis.
Robust scalarization	Maximize worst-case or quantile of $\mathcal{J}_{\mathrm{info}}$	Promotes stable, non-fragile perturbation patterns.

In continuous time, the reduced dynamics can be expressed in control-affine form with bounded nonlinearities,

$$\begin{aligned} \dot{x}(t) &= f\big(x(t),\theta\big) \quad + \quad G\big(x(t),\theta\big)\,u(t) \quad + \quad \xi(t) \\ y(t) &= h\big(x(t),\theta\big) \quad + \quad \varepsilon(t) \end{aligned} \tag{1}$$

where θ is a parameter vector, ξ is a bounded process disturbance capturing unmodeled effects, y collects measured outputs, and ε is measurement noise and bias. The outputs include surface casing pressure, standpipe pressure proxy, flow-out, and pit volume change [17]. The dependence on θ is explicit because identifiability is a central theme.

A key aspect is the representation of dissolution and swelling. Dissolution is modeled as a mass transfer between free and dissolved inventories driven by an equilibrium dissolved fraction that depends on pressure and temperature. Temperature is treated as a known bounded profile over the time horizon of interest, so its influence is embedded within the equilibrium mapping. The transfer is represented by a relaxation law at the reduced level,

$$\begin{aligned} \dot{M}_d(t) &= \kappa_d\Big(M_d^{\star}\big(p(t)\big) - M_d(t)\Big) \quad + \quad \eta_d(t) \\ \dot{M}_g(t) &= \dot{M}_{\mathrm{in}}(t) \quad - \quad \dot{M}_{\mathrm{out}}(t) \quad - \quad \kappa_d\Big(M_d^{\star}\big(p(t)\big) - M_d(t)\Big) \end{aligned} \tag{2}$$

where κ_d is an effective mass-transfer rate, $M_d^{\star}(p)$ is an equilibrium dissolved mass consistent with current pressure conditions, $\dot{M}_{\mathrm{in}}$ represents influx into the annulus when present, and $\dot{M}_{\mathrm{out}}$ represents surface outflow of free gas when present. The disturbance η_d captures the fact that reduced aggregation cannot perfectly represent the distributed dissolution process [18]. The equilibrium mapping $M_d^{\star}$ is derived from a bounded solubility mapping and an effective

TABLE 9: Numerical study scenarios and qualitative findings

Scenario	Regime	Goal	Key qualitative outcome
Swelling-dominated influx	Strong dissolution, small free gas	Separate influx magnitude from dissolution strength under pit ambiguity	Choke excitation reduces correlation between θ_k and θ_d.
Free-gas-dominated influx	Weak dissolution, larger free gas	Assess need for excitation when signatures are already strong	Robust information gain small; excitation can be reduced or skipped.
Friction change, no influx	Rising friction, no gas	Discriminate friction-induced pressure drops from kicks	Designed perturbations favor sensitivity directions orthogonal to θ_f.
Pit bias with swelling	Pit bias plus dissolution-driven gain	Separate swelling from inventory bias	Pressure-based excitation helps de-correlate bias and swelling parameters.
Property uncertainty	Variable compressibility and resistance	Test safety and informativeness under model mismatch	Robust design avoids near-boundary pressures and fragile perturbations.

liquid mass scale, ensuring that M_d remains bounded and that swelling does not become unphysical.

Swelling is represented through a state-dependent effective liquid density and volume mapping. The reduced model uses an effective swelling factor $B_l(\bar{x}_d)$ that modifies the mapping between liquid mass flow and volumetric flow at surface, and modifies the hydrostatic component of pressure distribution by changing effective density. In reduced form, the mapping enters as a correction to the pressure node dynamics and to the pit volume dynamics. The pit volume change is modeled as

$$\dot{V}_{\rm pit}(t) = Q_{\rm in}(t) \quad - \quad Q_{\rm out}(t) \tag{3}$$

with $Q_{\rm out}$ computed from mass flow and density so that swelling alters the volumetric return even without large free-gas outflow. The explicit inclusion of M_d and B_l is the mechanism by which swelling-driven pit gain is represented as an internal state effect rather than as measurement bias.

Pressure dynamics in reduced form must capture two coupled contributions: hydrostatic and frictional gradients, and compressible storage effects that govern transient response to actuation [19]. A low-order representation is used in which pressure nodes are connected by effective resistive and capacitive elements, yielding dynamics similar to a distributed RC network in hydraulic analogy. The resistive elements depend on friction parameters and mixture properties, while the capacitive elements depend on compressibility and effective storage. This yields a smooth dynamical system in which choke action modifies boundary pressure and thereby propagates into internal pressures with a time constant governed by compressibility and flow.

Influx is parameterized to make the identifiability question precise. Rather than treat influx as an arbitrary function, it is parameterized by a small set of parameters θ_k, such as onset time τ_k, a depth proxy mapped into the reduced model as an effective source location weight, and a rate magnitude and shape coefficient [20]. The resulting influx mass rate $\dot{M}_{\rm in}(t)$ is a smooth function of time with a small number of parameters. This parameterization is not claimed to represent all possible influx profiles; it is chosen because identifiability from surface signals is limited, and a low-dimensional parameterization aligns with that limit.

The overall parameter vector is then partitioned as $\theta = [\theta_k, \theta_f, \theta_s, \theta_d, \theta_b]$, where θ_f represents friction multipliers and flow-regime smoothing parameters, θ_s represents slip timing proxies that influence $\dot{M}_{\rm out}$ and the near-surface gas indicator, θ_d represents dissolution kinetics and swelling coefficients, and θ_b represents sensor bias parameters for pit and flow measurements. Identifiability questions are then stated as whether θ_k and θ_d can be distinguished from θ_f and θ_b given the measured outputs and admissible inputs.

This reduced formulation is designed to admit boundedness and smoothness, which is essential for Koopman lifting and for stable computation of information metrics. It also admits structured uncertainty, because property-model uncertainty can be represented as bounded perturbations

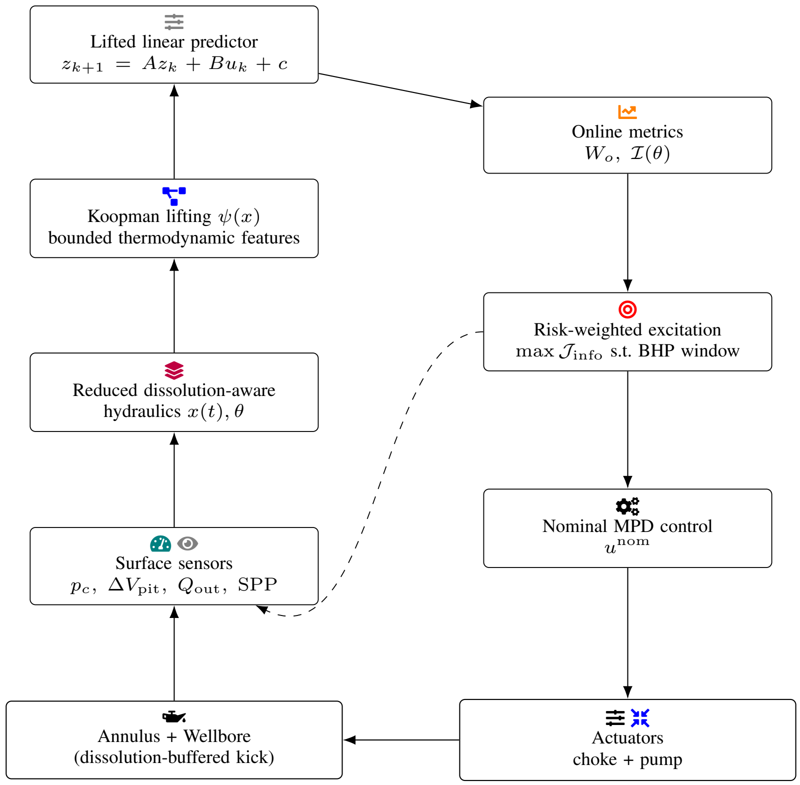

FIGURE 7: Observability-aware managed pressure drilling workflow for dissolution-buffered gas influx identification. Surface measurements are interpreted through a reduced dissolution-aware model and a Koopman-lifted linear predictor, enabling fast observability/Fisher-information surrogates that drive constrained, risk-weighted excitation around nominal MPD control.

of resistive and capacitive coefficients and of equilibrium solubility mapping. The reduced model is not intended to replace full simulation, but to serve as an information-structure model that captures the dominant modes by which surface measurements become informative about hidden gas states.

The question now becomes how to compute, in real time, which directions in θ are observable under a candidate input sequence [21]. Direct nonlinear observability analysis is not tractable online. The next section therefore develops a Koopman-lifted representation that yields a linear predictor in a lifted space, enabling tractable observability Gramian computation and a Fisher-information surrogate that can guide excitation design.

III. Koopman-Lifted Linear Predictors and Online Information Metrics

Koopman operator theory provides a way to represent nonlinear dynamics through linear evolution of observables. For a nonlinear discrete-time system $x_{k+1} = F(x_k, u_k)$, the Koopman operator acts on functions φ of the state by $(\mathcal{K}\varphi)(x) = \varphi(F(x, u))$ for fixed input. In practice, one constructs a finite-dimensional approximation by selecting a dictionary of observables and fitting a linear operator that advances those observables. For identification and observability analysis, the key advantage is that once a lifted linear system is available, classical linear-system tools become applicable, including observability Gramians and Fisher-information calculations, while nonlinearities remain embedded within the lifting map.

In this paper, the Koopman approach is used in a structured manner [22]. The lifting functions are not arbitrary nonlinear features; they are chosen to reflect the physics of dissolution-buffered influx. The lifted state includes the reduced state itself and additional nonlinear observables capturing bounded dissolved fraction, swelling factor, pressure-dependent compressibility proxies, and products that reflect coupling between gas inventory and pressure. Boundedness is enforced by using smooth saturating maps in the features, preventing the lifted predictor from producing unphysical divergence under input sequences that remain within operational bounds.

Let $\psi : \mathbb{R}^n \to \mathbb{R}^r$ denote the lifting map, with $r \gg n$ but still small enough for online computation. The lifted dynamics are approximated as

$$\begin{aligned} \psi(x_{k+1}) &= A(\theta)\,\psi(x_k) \quad + \quad B(\theta)\,u_k \quad + \quad c(\theta) \quad + \quad \omega_k \\ y_k &= C(\theta)\,\psi(x_k) \quad + \quad d(\theta) \quad + \quad \nu_k \end{aligned} \tag{4}$$

where A, B, C are fitted operators, c, d are affine offsets, and ω, ν represent approximation and measurement errors. The dependence on θ is emphasized because the objective is not merely prediction but information about parameters

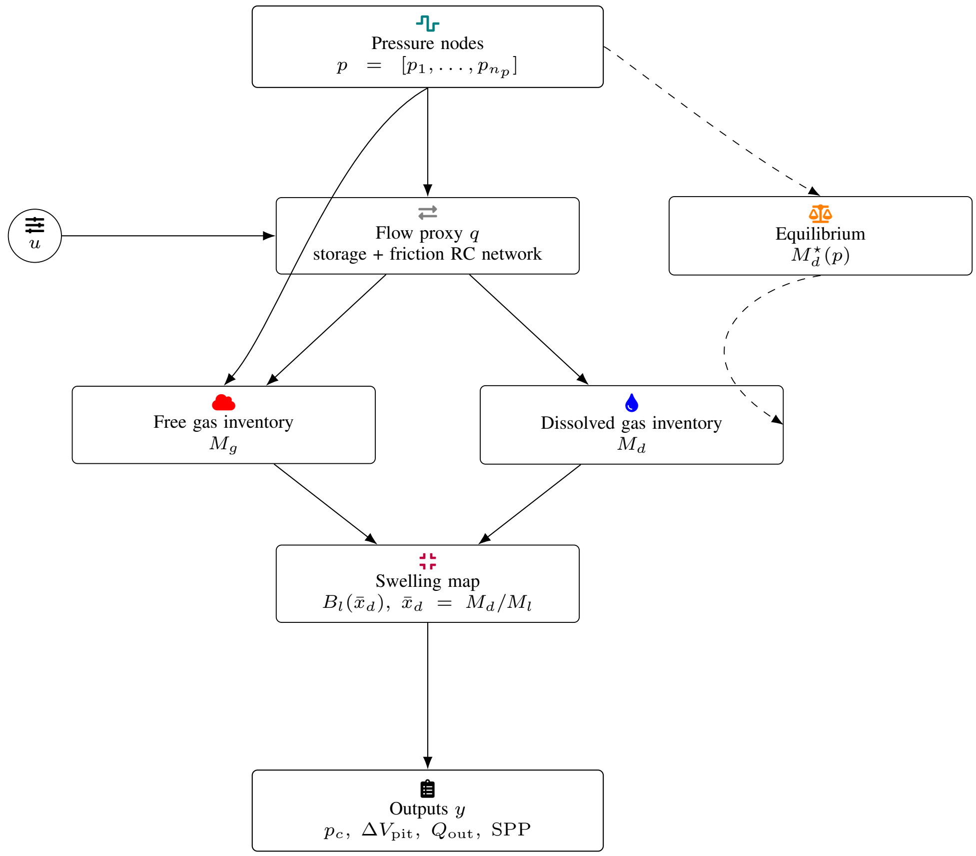

FIGURE 8: Reduced annular state coupling retained for identifiability: low-order pressure/flow dynamics interact with free and dissolved gas inventories through an equilibrium-driven dissolution transfer and a swelling-dependent volumetric map, shaping surface pit gain and pressure signatures without requiring a dominant free-gas phase.

[23]. Two practical constructions are used. In the first, separate lifted operators are learned for discrete parameter grid points, yielding an interpolated operator family. In the second, the operators are expressed as affine functions of a small subset of parameters, allowing gradients with respect to parameters to be computed directly. The second approach is preferred for online information metrics, but it requires that parameter dependence be sufficiently smooth over the operating envelope.

Training data for Koopman fitting is generated by simulating the reduced dissolution-aware model across a distribution of input sequences and parameter samples consistent with operational envelopes. The input sequences include typical managed pressure actions and also include small structured perturbations, because the goal is to evaluate the informational impact of such perturbations [24]. The training objective minimizes multi-step prediction error in lifted coordinates and output space, not just one-step error, because observability metrics depend on how outputs accumulate information over time. Regularization is applied to ensure that the lifted predictor remains stable under bounded inputs, for example by constraining the spectral radius of A in the mean sense and by penalizing growth in unforced trajectories. These constraints are operationally motivated: a predictor that is unstable in lifted space can yield misleading observability metrics by amplifying uninformative modes.

Once a lifted linear predictor is available, an observability Gramian can be computed for a given input sequence. For linear time-varying systems, observability depends on the sequence of output matrices and state transition matrices. In the lifted setting, the system is approximately linear time invariant under fixed θ and for inputs entering through B [25]. For a horizon N, the lifted observability Gramian is

$$W_o = \sum_{k=0}^{N-1} \left(A^\top\right)^k C^\top C A^k \tag{5}$$

in the simplest time-invariant case, with modifications when C depends on inputs or when a time-varying linearization is used. The Gramian provides a measure of how well the lifted state can be reconstructed from output history, but the primary interest here is not reconstructing $\psi(x)$ itself. Instead, the interest is in reconstructing specific parameter directions, such as influx magnitude and dissolution kinetics, from outputs. This motivates a Fisher-information surrogate [26].

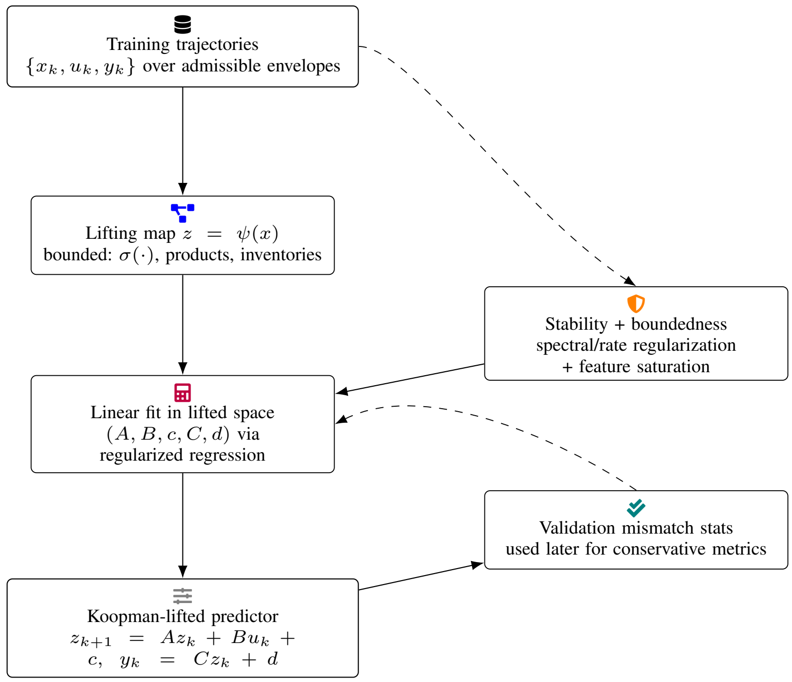

FIGURE 9: Structured Koopman construction for dissolution-buffered annular dynamics. Physics-motivated, bounded observables lift the reduced state to a space where a linear predictor is fitted with stability regularization, producing a fast surrogate whose validation mismatch is retained for conservative online information evaluation.

For a parameterized system with outputs $y_k(\theta)$ corrupted by Gaussian noise with covariance R, the Fisher information matrix over a horizon is approximately

$$\mathcal{I}(\theta) = \sum_{k=0}^{N} \left(\frac{\partial y_k}{\partial \theta}\right)^{\top} R^{-1} \left(\frac{\partial y_k}{\partial \theta}\right) \tag{6}$$

In the lifted predictor, $y_k = C\psi(x_k) + d$, and the state x_k evolves through the lifted system. Sensitivities can be computed by differentiating the lifted recursion with respect to θ, yielding a sensitivity system that is linear in the sensitivities. The key practical point is that this sensitivity computation is far cheaper in the lifted linear system than in the original nonlinear model, and it can be evaluated for many candidate input sequences during excitation design.

To maintain robustness under approximation error, the Fisher-information surrogate is regularized by adding a model discrepancy term. Specifically, the effective noise covariance is inflated by an amount that reflects the mismatch observed between the lifted predictor and the reduced model during validation [27]. This prevents the excitation optimizer from exploiting fragile predictor artifacts. The inflated covariance can be state dependent, increasing during regimes where dissolution switching or near-surface gas emergence introduces greater nonlinearity. The result is an information metric that remains conservative with respect to surrogate fidelity.

The information matrix is used to define scalar objectives that quantify how informative an input sequence is about selected parameters. Common scalarizations include the log-determinant, which reflects volume of the uncertainty ellipsoid, and the trace of the inverse, which reflects average variance. In this paper, the objective is chosen to emphasize influx magnitude and onset timing while also maintaining identifiability of dissolution kinetics sufficiently to avoid misattribution [28]. This is achieved by weighting parameter subsets within the Fisher-information matrix and by using a risk-weighted scalarization that penalizes information gain obtained through unsafe pressure excursions.

A central challenge is that dissolution and influx can be locally unidentifiable because both can influence pit gain through swelling and volumetric mapping. The lifted information framework addresses this by explicitly incorporating cross-sensitivities. If the information matrix indicates strong correlation between influx magnitude and swelling coefficient directions, then point estimation will be ill conditioned, and excitation design can target inputs that decorrelate these directions by changing pressure in a way that affects equilibrium dissolution more than it affects free-gas compressibility. The method therefore uses not only the magnitude of information but also the conditioning of the information matrix to decide whether an input sequence is useful. In practice, the objective includes a penalty for poor conditioning, which promotes excitation that yields more orthogonal sensitivity directions [29].

The Koopman-lifted framework also provides a natural way to incorporate constraints on physical admissibility. Because the lifting functions are bounded and because the

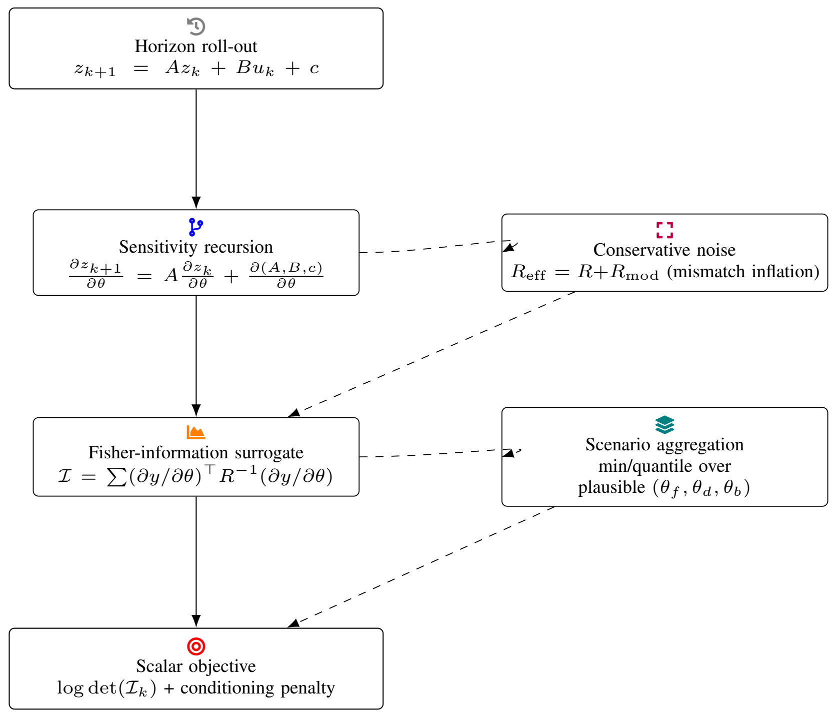

FIGURE 10: Online information computation enabled by the lifted linear predictor. Output sensitivities are propagated cheaply in lifted coordinates, assembled into a Fisher-information surrogate, and robustified via mismatch-inflated covariance and scenario-based aggregation to reduce over-optimistic excitation decisions.

lifted predictor is trained only on admissible trajectories, the predicted lifted states remain within a plausible region for bounded inputs. This does not guarantee physical admissibility in a strict sense, but it reduces the risk of generating excitation sequences that appear informative in the surrogate but would be invalid in the true system. This is complemented by explicit safety constraints enforced on predicted bottomhole pressure and other variables computed either from the reduced model directly or from a decoded surrogate mapping.

With observability and information metrics defined, the remaining step is to formulate and solve the excitation design problem. The next section develops a constrained receding-horizon excitation strategy that maximizes information subject to bottomhole-pressure window constraints and actuation limits, and that can be executed online alongside standard managed pressure control [30].

IV. Constrained Optimal Excitation Design under Pressure-Window Safety

Excitation design in drilling must respect the operational environment. It is not acceptable to apply arbitrary probing inputs, because bottomhole pressure must remain within a window, equipment limits must be respected, and operational continuity must be maintained. The objective is therefore not maximal information in an unconstrained sense, but maximal information within an admissible set of input trajectories that satisfy safety constraints and remain sufficiently smooth.

This section formulates the excitation design as a receding-horizon optimization that can be embedded as an additional layer in managed pressure workflows, producing small perturbations around a nominal control trajectory.

Let $u_k = u_k^{\text{nom}} + \delta u_k$, where u_k^{nom} is a nominal input sequence produced by the existing control system and δu_k is an excitation perturbation to be designed. The perturbations are constrained by amplitude and rate limits reflecting choke actuator bandwidth and pump constraints. The system predicted response under $u^{\text{nom}} + \delta u$ is evaluated using the Koopman-lifted predictor for information metrics and using a safety predictor for pressure constraints. Because safety constraints are critical, the design uses conservative predictions for bottomhole pressure, with uncertainty margins reflecting model mismatch and parameter uncertainty [31].

The optimization is posed over a horizon N as

$$\max_{\delta u_{0:N-1}} \quad \mathcal{J}_{\text{info}}\big(\delta u_{0:N-1}\big) \quad - \quad \lambda_u \sum_{k=0}^{N-1} \|\delta u_k\|^2 \tag{7}$$

subject to constraints that enforce safety and smoothness. The information objective $\mathcal{J}_{\text{info}}$ is derived from the Fisher-information surrogate for the parameter subset of interest. A log-determinant form is used for influx-related parameters to encourage volume reduction in uncertainty, while a conditioning penalty is added to discourage nearly singular information matrices. The quadratic penalty on δu discourages disruptive excitation and provides regularization.

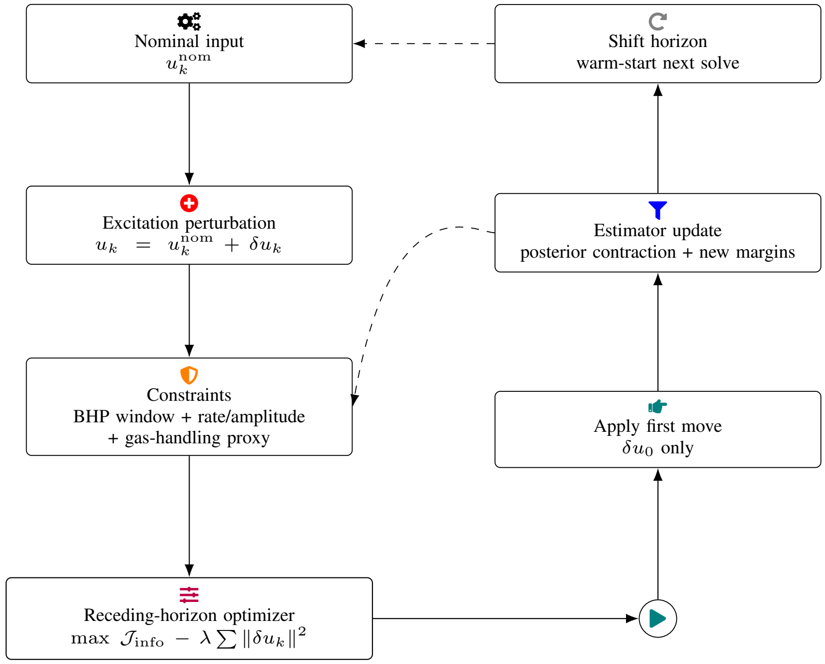

FIGURE 11: Constrained receding-horizon excitation design compatible with managed pressure drilling. A small perturbation is optimized for information gain under safety and actuator limits, applied in a first-move fashion, and iterated as estimates and safety margins adapt in real time.

Safety constraints enforce that predicted bottomhole pressure remains within the window with a conservative margin. Denote predicted bottomhole pressure as $\hat{p}_{\mathrm{bh},k}(\delta u)$ obtained from the reduced model or from a safety mapping trained to bound bottomhole pressure. The constraint is [32]

$$p_{\min} + m_k \le \hat{p}_{\mathrm{bh},k}(\delta u) \le p_{\max} - m_k \tag{8}$$

where m_k is a time-dependent safety margin that accounts for prediction error and uncertainty. The margin is increased when parameter uncertainty is large, reflecting that the same control action can produce a larger pressure response under different friction or compressibility conditions. As uncertainty contracts through ongoing estimation, the margin can decrease, allowing slightly richer excitation. This adaptive margin prevents the excitation design from being overly conservative at all times while maintaining protection when ambiguity is high.

Actuation constraints include amplitude bounds and rate bounds, [33]

$$\delta u_{\min} \le \delta u_k \le \delta u_{\max} \quad \text{and} \quad \|\delta u_k - \delta u_{k-1}\| \le r_{\max} \tag{9}$$

ensuring that the excitation is smooth and implementable. In practice, the excitation is often applied primarily through the choke because choke adjustments can modulate annular pressure without changing the primary circulation objectives. Pump excitation is used more sparingly because pump changes can affect cuttings transport and other operational objectives. The framework supports both, but the constraint weights can reflect operational preference.

Because the objective is nonlinear in δu through the information metric, direct global optimization is not required. The perturbations are small, and a local sequential quadratic programming approach suffices if gradients of the information metric with respect to δu are available [34]. The Koopman-lifted predictor provides these gradients efficiently because sensitivities propagate linearly in lifted space. The safety predictor can also provide gradients if differentiable, or it can be enforced using conservative linear constraints derived from bounded sensitivity estimates. The combination yields an optimization that can be solved online with warm starts.

An important aspect is the interplay between dissolution and excitation. To distinguish dissolution-driven swelling from free-gas expansion, the excitation should alter pressure in a way that changes equilibrium solubility and thus changes the dissolved inventory. A choke perturbation that increases pressure tends to increase solubility, encouraging dissolution and reducing free gas locally, which should reduce near-surface gas indicators while potentially increasing swelling effects in the liquid return [35]. Conversely, a pressure decrease encourages exsolution, potentially increasing free gas. The resulting differential response across pit volume, flow-out, and pressure signals provides information about dissolution kinetics and equilibrium strength. The excitation design objective implicitly captures this through the sensitivity structure; it does not need explicit heuristic rules about “test pulses.” Instead, the optimizer chooses the perturbation shape that maximizes information subject to constraints.

The excitation design is implemented in a receding-horizon manner. At each update time, current parameter uncertainty is represented by a covariance or by a local approximation derived from recent estimation. The information metric is evaluated around the current estimate, and a perturbation sequence is optimized [36]. Only the first perturbation is applied, then the horizon shifts. This allows the design to adapt as conditions evolve and as uncertainty contracts. It also allows the design to stop excitation when sufficient identifiability is achieved or when operational conditions change such that excitation is undesirable.

A key design decision is how to avoid inadvertently increasing risk while seeking information. The safety margins address pressure risk, but surface handling risk must also be considered. In dissolution-buffered regimes, excitation that decreases pressure could induce exsolution and increase free gas, potentially raising surface gas fraction [37]. Therefore, a secondary constraint is included on predicted surface gas handling proxy, such as near-surface free-gas fraction or gas outflow rate. This constraint is treated conservatively because it is less directly measured than pressure. The excitation optimizer then avoids perturbations that would likely trigger large exsolution near surface, unless such perturbations are unavoidable for identifiability and can be executed safely.

The excitation design does not replace managed pressure control; it augments it. The nominal control continues to regulate pressure and flow according to operational objectives. The excitation is designed to be small, structured, and transient, with the goal of improving inference rather than changing the operating point [38]. In this sense, the method functions as an observability-aware layer that can be activated when ambiguity is high and deactivated when the system is sufficiently identified.

The next section addresses robustness. Information metrics derived from a surrogate can be fragile if model mismatch is ignored. Property uncertainty and sensor bias can also distort information calculations by changing sensitivities. The following section therefore develops robust information evaluation that accounts for bounded uncertainty and bias, ensuring that excitation decisions are not driven by overly optimistic surrogate predictions [39].

V. Robust Information Evaluation under Property Uncertainty and Sensor Bias

A purely nominal Fisher-information computation can be misleading in drilling because the true system can deviate from nominal predictions due to PVT uncertainties, friction variations, slip regime changes, and sensor bias. If excitation design is driven by a nominal information metric, it may target parameter directions that are theoretically identifiable in the nominal model but practically confounded in the true system. Robust excitation design therefore requires that information be evaluated in a way that accounts for uncertainty in both dynamics and measurements.

The framework adopts a local robust information evaluation based on uncertainty propagation in the lifted predictor. Parameter uncertainty is represented by a covariance matrix P_θ for the parameters being estimated and by bounded intervals for nuisance uncertainties that are not explicitly estimated at the moment, such as short-term friction fluctuation. Sensor bias is represented as additional parameters with priors or as bounded offsets with slow dynamics [40]. The Koopman-lifted predictor supports these representations because it provides explicit sensitivities of outputs with respect to parameters and because it is fast enough to evaluate multiple uncertainty scenarios.

Robustness is introduced through two complementary mechanisms. The first is covariance inflation in the information calculation. The effective measurement noise covariance R is augmented by a model discrepancy covariance R_{mod} that accounts for surrogate error and unmodeled variability. This yields an effective noise $R_{\mathrm{eff}} = R + R_{\mathrm{mod}}$, reducing the nominal information. The discrepancy term is not arbitrary; it is constructed from validation error statistics of the lifted predictor and can be state dependent, increasing during regimes where dissolution switching is active. The effect is to prevent the excitation optimizer from seeking information through fragile dynamics where the predictor error would dominate.

The second mechanism is scenario-based information evaluation [41]. Instead of computing $\mathcal{I}(\theta)$ at a single nominal θ, the method computes information across a small set of representative parameter scenarios drawn from the current uncertainty, including variations in friction and dissolution strength that are plausible. The robust objective then aggregates these information matrices conservatively, for example by maximizing the minimum information over scenarios or by maximizing a quantile. This ensures that the excitation provides information across plausible models, not only in the nominal. Because the lifted predictor is fast, scenario evaluation is feasible online with a small scenario count.

Sensor bias is a particularly important confounder for pit-volume based inference. A persistent pit bias can mimic swelling-driven pit gain or can mask a small swelling effect. Therefore, bias parameters are included in the sensitivity structure [42]. If bias is not modeled, the information metric can incorrectly attribute sensitivity to dissolution parameters when in fact pit changes are dominated by bias uncertainty. Including bias causes the information matrix to reflect the trade-off: if pit bias is large, pit-based information about dissolution is reduced unless additional signals or excitation reduces bias uncertainty. This encourages excitation that leverages pressure measurements, which are often less biased, to improve dissolution identifiability indirectly through equilibrium response, rather than relying on pit signals alone.

Property uncertainty influences information because it changes the mapping from pressure to density and thus changes how pressure transients propagate and how swelling affects hydrostatics. In the reduced model, these uncertainties appear as perturbations to effective resistances and capacitances. In lifted space, these uncertainties are represented as additional parameters or as bounded disturbances [43].

Robust information evaluation accounts for them by inflating uncertainty in predicted outputs and by considering scenario variations. This is particularly relevant when attempting to identify influx magnitude from pressure drops, because friction uncertainty can produce similar pressure drops. Robust information evaluation thus tends to reduce apparent information in such confounded regimes, which is desirable because it prevents overconfident inference.

The robustness mechanisms also support stability of excitation design. If the information objective is highly sensitive to small model changes, the optimizer can produce erratic excitation sequences that switch rapidly between patterns. By evaluating robust information, the objective becomes smoother with respect to excitation, promoting more consistent perturbations [44]. Rate constraints further dampen excitation variability. The result is an excitation strategy that is stable and operationally acceptable.

Robust evaluation must also respect bounded thermodynamic behavior. Dissolution equilibrium mappings and swelling factors must remain bounded, and their uncertainty must be coupled rather than independent to avoid inconsistent extremes. The reduced model representation couples these uncertainties through shared coefficients, ensuring that a scenario with high solubility also implies higher swelling within plausible bounds, rather than allowing a physically inconsistent combination that would exaggerate ambiguity [45]. This coupling is important because otherwise robust evaluation could become overly conservative by considering extremes that cannot co-occur physically.

The outcome of robust information evaluation is an information metric that provides a conservative estimate of how much the excitation will reduce uncertainty in influx and dissolution parameters. This metric can be used to decide whether excitation is worthwhile. If robust information gain is small, the system may choose to avoid excitation and rely on passive monitoring, because excitation would introduce operational disruption without meaningful identifiability improvement. Conversely, if robust information gain is large, the system can justify excitation as a bounded-risk action that improves diagnostic clarity.

The next section presents numerical studies evaluating the proposed approach [46]. The emphasis is on how excitation changes identifiability in swelling-dominated regimes, how robust information avoids misleading excitation under property uncertainty, and how the method can be integrated into real-time workflows without requiring high-dimensional simulation.

VI. Numerical Studies: Identifiability Gains from Safe Excitation in Swelling-Dominated Regimes

The numerical evaluation is structured to isolate the information-theoretic effects of excitation rather than to demonstrate a specific well configuration. The studies use a representative reduced annular model calibrated to typical managed pressure drilling response scales, with outputs resembling surface casing pressure, standpipe pressure proxy, flow-out, and pit volume change. The parameter uncertainties include influx magnitude and onset time, dissolution kinetics and swelling coefficients, friction multipliers, and pit bias. Property-model uncertainty is represented as bounded variations in effective compressibility and resistance parameters, reflecting plausible correlation deviations.

The first study examines a swelling-dominated early influx in which a small gas influx occurs at depth under high pressure and dissolves substantially, producing pit gain primarily through swelling rather than through free-gas holdup [47]. Under a nominal managed pressure control trajectory with no deliberate excitation, the measured signals exhibit a slow pit rise and modest pressure changes that are consistent with multiple explanations: a small influx with strong dissolution, a slightly larger influx with weaker dissolution, or a friction change coupled with pit bias. A conventional estimator operating on these signals can produce a posterior that is elongated along a correlated direction between influx magnitude and dissolution strength, indicating that the system is poorly identifiable.

The excitation layer is then activated. The designed perturbation consists of a small-amplitude, smooth choke modulation over a short interval, constrained so that bottomhole pressure remains within the window with a conservative margin. The perturbation is selected by maximizing a robust Fisher-information objective weighted toward influx magnitude and dissolution kinetics. The key observation is that this modulation changes pressure sufficiently to alter equilibrium dissolution and thus produces a differential response across pit and pressure signals that is not produced by friction variation alone [48]. When the system is dissolution-buffered, the pit response shows a characteristic phase-lagged change consistent with dissolution kinetics, while pressure measurements respond more immediately. When the system is free-gas dominated, the modulation produces a different coupling pattern between pressure and flow-out. The information calculation captures these differences through sensitivities.

After applying the first perturbation, the estimator updates the parameter uncertainty using the new data, and the posterior contracts. The contraction is measured in terms of the determinant of the estimated covariance restricted to influx parameters, as well as in terms of the correlation between influx magnitude and dissolution parameters. The results show that, in swelling-dominated regimes, excitation can reduce this correlation substantially, producing a more identifiable parameter set [49]. The key point is not that uncertainty vanishes, but that ambiguity is reduced enough to support more confident discrimination between a benign swelling-driven pit gain and a free-gas-dominated scenario that would imply earlier surface gas risk.

The second study examines a free-gas-dominated influx where dissolution is weak or kinetics are slow. In this case, passive monitoring already provides relatively strong information because free gas affects pressure and flow-out in a more direct way. The excitation layer still computes a candidate perturbation, but robust information gain is smaller because the system is already more observable. The framework therefore either applies a smaller perturbation or chooses not to excite, depending on a threshold on expected robust information gain. This illustrates a practical principle: excitation is most valuable in regimes where the system is ambiguous, such as dissolution-buffered early events, and it is less necessary when conventional signatures already separate scenarios [50].

The third study focuses on the confounding effect of friction uncertainty. A scenario is simulated with no influx but with a friction increase due to changes in cuttings loading. This friction change produces a pressure signature that could be misinterpreted as an influx if considered in isolation. Under passive monitoring, the information matrix may suggest some sensitivity of outputs to influx parameters because the model allows influx as an explanation. The excitation layer is designed to discriminate: a pressure modulation induced by choke perturbation affects dissolution equilibrium and gas inventory only if gas is present, whereas a friction change responds differently [51]. The robust information objective thus tends to select perturbations that amplify differences in sensitivity between gas-related parameters and friction parameters. The result is that, after excitation, the measurement-consistent set of parameters can rule out influx explanations more strongly, reducing false alarm likelihood.

The fourth study evaluates robustness under sensor bias. Pit bias is introduced as an unknown offset and slow drift. Under passive monitoring, pit gain becomes unreliable for distinguishing swelling from bias. The robust information metric accounts for bias uncertainty and therefore reduces the apparent information contributed by pit measurements unless pressure and flow signals can support the distinction [52]. Excitation that modulates pressure becomes more valuable because it generates a pit response that depends on dissolution kinetics rather than on static bias, enabling bias and swelling to be separated in the estimation. The study shows that when bias is explicitly modeled, excitation is targeted differently than when bias is ignored, and the resulting inference is more consistent across sensors.

The fifth study examines the effect of property-model uncertainty on excitation selection. When compressibility and resistance parameters vary within bounds, the nominal predicted sensitivity of bottomhole pressure to choke perturbation can vary. If excitation were designed on a nominal model, it might inadvertently approach the pressure window boundary under an unfavorable parameter realization. The robust excitation design uses conservative margins and scenario-based safety evaluation, preventing such near-boundary actions [53]. At the same time, robust information evaluation avoids overvaluing perturbations that are informative only in the nominal scenario but not across plausible parameter variations. The study shows that robust design yields slightly smaller information gain per perturbation than nominal design, but it avoids unsafe or misleading perturbations and yields more consistent posterior contraction.

Across studies, a recurring observation is that the excitation patterns selected by the optimization are not arbitrary oscillations but structured perturbations aligned with the system's natural time scales. Perturbations are slow enough to be tracked by choke hardware and to avoid inducing high-frequency pressure waves that could be operationally undesirable, yet fast enough to create a measurable differential response before the system evolves significantly due to migration. This alignment emerges naturally from the constraints and from the sensitivity structure, rather than being imposed as a heuristic rule.

The numerical results also highlight limits [54]. If the pressure window is extremely narrow, safety margins may preclude any meaningful excitation, and the system remains ambiguous. In such cases, the framework correctly indicates low robust information gain and avoids applying perturbations that would not improve identifiability. If sensors are insufficient, for example if flow-out measurement is unreliable and pit bias is large, identifiability remains limited even with excitation. The method does not eliminate the need for adequate sensing; it provides a principled way to quantify when sensing and excitation are sufficient and when they are not.

Finally, it is important to interpret the Koopman-lifted information metrics as operational approximations rather than exact guarantees. Their value lies in providing a computationally tractable, structured estimate of information content that can guide excitation decisions [55]. The studies indicate that these metrics correlate with observed posterior contraction in the reduced model setting, and that robust variants remain stable under uncertainty. This supports the use of the method as an observability-aware layer that can be integrated into real-time workflows.

VII. Conclusion

This paper developed an observability-centered framework for dissolution-buffered gas influx identification in managed pressure drilling by combining a dissolution-aware reduced annular model with Koopman-lifted linear predictors and constrained optimal excitation design. The approach was motivated by the structural ambiguity introduced by dissolution-driven swelling and by the confounding influence of friction and property uncertainties on surface measurements. Rather than treating inference as a purely statistical detection task, the method explicitly targeted the information limitation by computing lifted observability and Fisher-information surrogates and by designing small, admissible input perturbations that increase identifiability while respecting bottomhole-pressure window constraints and actuator limits.

The technical contributions were a structured lifting design that embeds bounded dissolution and swelling observables, an online-computable information metric that accounts for surrogate discrepancy and nuisance uncertainties, and a receding-horizon excitation optimization that balances information gain against operational disruption and risk [56]. Numerical studies showed that, in swelling-dominated regimes where pit gain is intrinsically ambiguous, modest choke perturbations can reduce correlation between influx magnitude and dissolution parameters, producing more decisive posterior contraction than passive monitoring. Robust evaluation under property uncertainty and sensor bias prevented misleading excitation choices and supported stable operation within conservative safety margins.

The framework is intended to complement, not replace, existing managed pressure control and monitoring systems. Its practical role is to identify when the system is poorly observable, to quantify which parameter directions are ambiguous, and to propose safe, structured excitation that reduces that ambiguity. Future extensions can incorporate richer temperature representations when thermal variation materially affects solubility on the relevant time scale, and can refine lifting dictionaries to better capture regime-dependent slip effects while retaining boundedness and stability. Within these bounds, the proposed Koopman-lifted excitation design provides a practical path to make dissolution-aware influx identification more reliable by treating observability and excitation as first-class components of the real-time workflow [57].

REFERENCES

[1] P. G. Lillis, J. Palacas, and A. Warden, "A precambrian-cambrian oil play in southern utah," *AAPG Bulletin*, vol. 79, 6 1995.

[2] A. Tallin, P. Paslay, E. P. Cernocky, and M. A. Ratchinsky, "Risk assessment of exploration well designs in the oman ara salt," in *SPE Annual Technical Conference and Exhibition*, SPE, 10 2000.

[3] L. Blecha, T. J. Cox, A. Loeb, and L. Hernquist, "Recoiling black holes in merging galaxies: Relationship to agn lifetimes, starbursts, and the m-sigma relation," *Monthly Notices of the Royal Astronomical Society*, vol. 412, pp. 2154–2182, 1 2011.

[4] K. Manikonda, A. R. Hasan, O. Kaldirim, N. Rahmani, and M. A. Rahman, "Estimating swelling in oil-based mud due to gas kick dissolution," in *International conference on offshore mechanics and arctic engineering*, vol. 84430, p. V011T11A039, American Society of Mechanical Engineers, 2020.

[5] K. Manikonda, A. R. Hasan, N. H. Rahmani, O. Kaldirim, C. E. Obi, J. J. Schubert, and M. A. Rahman, "A gas kick model that uses the thermodynamic approach to account for gas solubility in synthetic-based mud," in *SPE/IADC Middle East drilling Technology conference and exhibition*, p. D031S016R001, SPE, 2021.

[6] B. A. Elieff and J. Schubert, "Dual gradient drilling will control shallow hazards in deepwater environments," in *Volume 7: Offshore Geotechnics; Petroleum Technology*, pp. 509–539, ASMEDC, 1 2009.

[7] V. Casariego, "Generation, migration, and transportation of gas contaminated regions of drilling fluid.," 1 1987.

[8] J. Nunes, A. C. Bannwart, and P. Ribeiro, "Mathematical modeling of gas kicks in deep water scenario," in *IADC/SPE Asia Pacific Drilling Technology*, SPE, 9 2002.

[9] A. K. Sleiti, W. A. Al-Ammari, M. Abdelrazeq, M. El-Naas, M. A. Rahman, A. Barooah, R. Hasan, and K. Manikonda, "Comprehensive assessment and evaluation of correlations for gas-oil ratio, oil formation volume factor, gas viscosity, and gas density utilized in gas kick detection," *Journal of Petroleum Science and Engineering*, vol. 207, p. 109135, 2021.

[10] D. Maldonado-Mundo, L. He, P. Öhberg, and M. Valiente, "Non-galilean response of rashba-coupled fermi gases," *Physical Review A*, vol. 88, pp. 053609–, 11 2013.

[11] G. C. Yang, H. J. Zhang, J. Epp, and S. W. Nas, "Managed pressure drilling micro flux technology allows safer drilling in highly sour reservoirs.," in *International Oil and Gas Conference and Exhibition in China*, SPE, 6 2010.

[12] M. Yousif and D. Young, "A simple correlation to predict the hydrate point suppression in drilling fluids," *SPE/IADC Drilling Conference*, 2 1993.

[13] D. Okba, "Saharan aquifers protection in oil and gas upstream activities in algeria: A sustainable-development challenge," in *International Petroleum Technology Conference*, IPTC, 11 2005.

[14] A. Lantz, J. Larfeldt, A. Ehn, J. Zhu, A. A. Subash, E. J. Nilsson, Z. Li, and M. Aldén, "Investigation of ozone stimulated combustion in the sgt-800 burner at atmospheric conditions," in *Volume 4A: Combustion, Fuels and Emissions*, American Society of Mechanical Engineers, 6 2016.

[15] A. Hashim and Z. Yasin, "Overview of acid stimulation practices in malaysian oil fields," in *SPE Asia Pacific Oil and Gas Conference*, SPE, 2 1993.

[16] A. Sonde, U. Ozoemene, U. Nwabudike, F. Ifeanyi-Onah, O. Amuboh, and M. Esho, "Improving value by leveraging on integrated multi-discipline data review for a partially appraised gas field development: The zed field case study," in *SPE Nigeria Annual International Conference and Exhibition*, SPE, 8 2015.

[17] R. Guo, Y. Chen, R. P. Coutinho, and P. J. Waltrich, "Numerical and experimental investigations of gas kick migration during casing while drilling," in *SPE Health, Safety, Security, Environment, & Social Responsibility Conference - North America*, SPE, 4 2017.

[18] G. Palasthy, V. Pipicz, I. Munkacsi, and S. Tromboczky, "Horizontal wells in the algyo field, hungary-evaluation of a successful ior project," in *SPE/DOE Improved Oil*

Recovery Symposium, pp. 407–414, SPE, 4 1998.

[19] C. Wei and Y. Chen, "On improving algorithm efficiency of gas-kick simulations toward automated influx management: A robertson differential-algebraic-equation problem approach," *SPE Drilling & Completion*, vol. 36, pp. 943–966, 10 2021.

[20] . J. staff, "Ec-drill eliminates effect of equivalent circulating density," *Journal of Petroleum Technology*, vol. 65, pp. 38–40, 8 2013.

[21] R. Samuel, "Kick detection using downhole accelerometer data," *Journal of Energy Resources Technology*, vol. 142, 5 2020.

[22] G. Flatabø, A. Torsvik, V. M. Oltedal, B. J. Bjørkvik, A.-A. Grimstad, and H. Linga, "Experimental gas absorption in petroleum fluids at hpht conditions," in *SPE Bergen One Day Seminar*, SPE, 4 2015.

[23] Y. Mumtaz, A. U. Rehman, and M. J. Shaikh, "Simulation model for optimization of gas production system through integration of sub-surface and surface facilities," in *Abu Dhabi International Petroleum Exhibition & Conference*, SPE, 11 2018.

[24] L. Oyarte-Gálvez and D. van der Meer, "Granular motor in the non-brownian limit," *Journal of Statistical Mechanics: Theory and Experiment*, vol. 13, pp. 043206–, 4 2016.

[25] J. J. Chineke, T. Alabi, and H. D. Okwa, "Cost saving through casing design optimization ala-3 as case study," in *SPE Nigeria Annual International Conference and Exhibition*, SPE, 8 2021.

[26] T. Bayer, B. V. Cunning, R. Selyanchyn, M. Nishihara, S. Fujikawa, K. Sasaki, and S. M. Lyth, "Proton conduction in nanocellulose - paper fuel cells," *ECS Meeting Abstracts*, vol. MA2016-02, pp. 2603–2603, 9 2016.

[27] D. Sijacki, V. Springel, and M. G. Haehnelt, "Gravitational recoils of supermassive black holes in hydrodynamical simulations of gas-rich galaxies," *Monthly Notices of the Royal Astronomical Society*, vol. 414, pp. 3656–3670, 5 2011.

[28] B. W. McDaniel, L. E. East, M. J. Rosato, and M. Farabee, "Packerless multistage fracture-stimulation method using ct perforating and annular path pumping," in *SPE Annual Technical Conference and Exhibition*, SPE, 10 2005.

[29] H. Nickens, "A dynamic computer model of a kicking well: Part ii-model predictions and conclusions," *SPE Annual Technical Conference and Exhibition*, 9 1985.

[30] A. F. Ibrahim, M. Ibrahim, and C. Pieprzica, "Developing a new workflow to study the effect of soaking process on shale well," in *SPE Eastern Regional Meeting*, SPE, 10 2019.

[31] J. E. Chirinos, J. R. Smith, and D. A. Bourgoyne, "A simplified method to estimate peak casing pressure during mpd well control," in *SPE Annual Technical Conference and Exhibition*, SPE, 10 2011.

[32] K. Speirs, "Energy efficiency assessments - just a paper exercise?," in *SPE International Conference on Health, Safety, and Environment in Oil and Gas Exploration and Production*, SPE, 4 2008.

[33] H. Santos, E. Catak, J. I. Kinder, and P. Sonnemann, "Kick detection and control in oil-based mud: Real well test results using micro-flux control equipment," *SPE/IADC Drilling Conference*, 2 2007.

[34] W. J. Al-Mudhafar and A. K. Wojtanowicz, "A comparison simulation study of gdws-agd eor process performance using co2/apg alternatives in south rumaila oil field, iraq," in *SPE Improved Oil Recovery Conference*, SPE, 8 2020.

[35] R. Green and C. Korzekwa, "Dewatering a deep gas well with a gas lift system-a case history," in *Permian Basin Oil and Gas Recovery Conference*, SPE, 3 1984.

[36] R. A. Shishavan, C. Hubbell, H. D. Perez, J. D. Hedengren, and D. S. Pixton, "Combined rate of penetration and pressure regulation for drilling optimization by use of high-speed telemetry," *SPE Drilling & Completion*, vol. 30, pp. 17–26, 3 2015.

[37] D. Denney, "Dynamic simulation establishes water-cut limits for well kickoff," *Journal of Petroleum Technology*, vol. 57, pp. 64–65, 5 2005.

[38] K. Ketata, M. Ketata, S. Koumetz, and J. Marcon, "Beryllium diffusion mechanisms in ingaas compounds grown by gas source molecular beam epitaxy," *Europhysics Letters (EPL)*, vol. 45, pp. 348–353, 2 1999.

[39] T. Jacobs, "Innovators seek to transform flaring into money and power," *Journal of Petroleum Technology*, vol. 72, pp. 24–29, 3 2020.

[40] A. Bourgoyne, O. Kelly, and C. Sandoz, "New ideas for shallow gas well control," 6 1996.

[41] T. Hansen, "Projects of the year," *Power Engineering*, vol. 110, 1 2006.

[42] Y. Susilo, Z. Rahamanda, W. Wibowo, R. Tjahyadi, F. J. Silitonga, and I. Nasser, "Stimulation efforts in carbonate gas reservoir experiencing subsidence in offshore north west java field - indonesia," in *SPE Latin American and Caribbean Petroleum Engineering Conference*, SPE, 4 2003.

[43] H. Bagheri, A. A. Tanha, F. D. Ardejani, M. Heydari-Tajareh, and E. Larki, "Geomechanical model and wellbore stability analysis utilizing acoustic impedance and reflection coefficient in a carbonate reservoir," *Journal of Petroleum Exploration and Production Technology*, vol. 11, pp. 3935–3961, 9 2021.

[44] W. Liu, S. Lin, Y. Zhou, and S. Fang, "The successful application of a new-style managed pressure drilling mpd equipment and technology in well penglai 9 of sichuan & chongqing district," in *IADC/SPE Asia Pacific Drilling Technology Conference and Exhibition*, SPE, 7 2012.

[45] M. A. Diop, M. Fafard, and Z. Shi, "Numerical and experimental evaluations of cooling strategies and en-

vironmental sustainability for the cut-out aluminum reduction pot," *Journal of Sustainable Metallurgy*, vol. 7, pp. 718–731, 6 2021.

[46] O. Rauf, S. Gerdes, and N. R. Lummer, "Foam and scale inhibitor squeeze with natural gas: A lifeline for water flooded & damaged gas wells," in *SPE European Formation Damage Conference & Exhibition*, SPE, 6 2013.

[47] J. Schubert, H. C. Juvkam-Wold, J. Choe, and D. T. Dreher, "Analysis of gas kicks in multilateral wells utilizing computer simulation," *IADC/SPE Drilling Conference*, 2 2006.

[48] J. Vozniak, W. Dooley, R. Casto, G. Bologna, T. Beal, and K. Smejkal, "Successful west delta block 89 redevelopment utilizing re-entries and openhole horizontal gravel packing," in *SPE Annual Technical Conference and Exhibition*, SPE, 10 2000.

[49] D. Dupuis and S. Hancock, "Ad equation between a second generation semi and drilling extended-reach well in tunisia," *IADC/SPE Drilling Conference*, 3 2008.

[50] Q. Gu, A. Fallah, A. Ambrus, Z. Ma, D. Chen, P. Ashok, and E. van Oort, "A switching mpd controller for mitigating riser gas unloading events in offshore drilling," *SPE Drilling & Completion*, vol. 35, pp. 201–217, 1 2020.

[51] D. Denney, "Wellbore-stability assessment for self-killing blowouts," *Journal of Petroleum Technology*, vol. 65, pp. 105–110, 1 2013.

[52] E. Vefring, R. Rommetveit, and E. Borge, "An advanced kick simulator operating in a user-friendly x-window system environment," in *Petroleum Computer Conference*, SPE, 6 1991.

[53] J. Guedes, P. Madau, M. Kuhlen, J. Diemand, and M. Zemp, "Simulations of recoiling massive black holes in the via lactea halo," *The Astrophysical Journal*, vol. 702, pp. 890–900, 8 2009.

[54] Z. Xu, X. Chen, X. Song, Z. Zhu, and W. Zhang, "Gas-kick simulation in oil-based drilling fluids with nonequilibrium gas-dissolution and -evolution effects," *SPE Journal*, vol. 26, pp. 2549–2569, 7 2021.

[55] T. H. N. Tat, D. Gomes, and K. K. Fjelde, "Use of a transient model for studying kick migration velocities and build-up pressures in a closed well," in *Volume 10: Petroleum Technology*, American Society of Mechanical Engineers, 6 2021.

[56] P. Shrivastav, "An integrated approach towards well control of a hpht well," in *Offshore Technology Conference*, OTC, 4 2012.

[57] M. Suezawa, "Hydrogen-point defect complexes in electron-irradiated c-doped and high-purity si," *Japanese Journal of Applied Physics*, vol. 38, pp. 608–610, 6 1999.